



**Repositorio Institucional de la Universidad Autónoma de Madrid**

<https://repositorio.uam.es>

Esta es la **versión de autor** del artículo publicado en:

This is an **author produced version** of a paper published in:

Autophagy 11.6 (2015): 918-927

**DOI:** 10.1080/15548627.2015.1034413

**Copyright:** © 2015 Taylor & Francis

El acceso a la versión del editor puede requerir la suscripción del recurso

Access to the published version may require subscription

**TipC and the chorea-acanthocytosis protein VPS13A regulate autophagy in *Dictyostelium* and human HeLa cells**

**Sandra Muñoz-Braceras, Rosa Calvo and Ricardo Escalante\***

Instituto de Investigaciones Biomédicas Alberto Sols; C.S.I.C./U.A.M.; Madrid, Spain

\*To whom correspondence should be addressed: Instituto de Investigaciones Biomédicas Alberto Sols; C.S.I.C./U.A.M.; 28029 Madrid, Spain. Tel.: +34 915854467; E-mail: rescalante@iib.uam.es

**Running Title:** VPS13A regulates autophagy

**Keywords:** Autophagy, Chorea-acanthocytosis, Chorein, *Dictyostelium*, HeLa cells, TipC, VPS13, VPS13A.

**Abbreviations:** #*ATG*, autophagy-related; AX4, Axenic strain 4; DUF, domain of unknown function; GFP, green fluorescent protein; LC3, microtubule-associated protein 1 light chain 3; PtdIns3K, phosphatidylinositol 3-kinase; PtdIns3P, phosphatidylinositol 3-phosphate; VPS13, vacuolar protein sorting 13 homolog (*S. cerevisiae*); WIPI, WD repeat domain, phosphoinositide interacting

## Abstract

Deficient autophagy causes a distinct phenotype in *Dictyostelium discoideum*, characterized by the formation of multitips at the mound stage. This led us to analyze autophagy in a number of multitipped mutants described previously (*tipA*<sup>-</sup>, *tipB*<sup>-</sup>, *tipC*<sup>-</sup>, and *tipD*<sup>-</sup>). We found a clear autophagic dysfunction in *tipC*<sup>-</sup> and *tipD*<sup>-</sup> while the others showed no defects. *tipD* codes for a homolog of Atg16, which confirms the role of this protein in *Dictyostelium* autophagy and validates our approach. The *tipC*-encoded protein is highly similar to human VPS13A (also known as Chorein), whose mutations cause the chorea-acanthocytosis syndrome. No member of the VPS13 protein family has been previously related to autophagy despite the presence of a region of similarity to Atg2 at the C terminus. This region also contains the conserved domain of unknown function DUF1162. Of interest, the expression of the TipC C-terminal coding sequence containing these 2 motifs largely complemented the mutant phenotype. *Dictyostelium* cells lacking TipC displayed a reduced number of autophagosomes visualized with the markers GFP-Atg18 and GFP-Atg8 and an impaired autophagic degradation as determined by a proteolytic cleavage assay. Downregulation of human *VPS13A* in HeLa cells by RNA interference confirmed the participation of the human protein in autophagy. VPS13A-depleted cells showed accumulation of autophagic markers and impaired autophagic flux.

## Introduction

*Dictyostelium discoideum* is a social amoeba whose developmental process depends on macroautophagy (referred to as 'autophagy' hereafter for simplicity). This process is a highly conserved lysosomal degradation pathway and it is the main cellular mechanism for protein and organelle degradation in eukaryotes.<sup>1,2</sup> It is characterized by the formation of double membrane vesicles, the autophagosomes, which engulf a variety of cargos including portions of the cytoplasm, protein aggregates or damaged organelles. The autophagosomes eventually fuse with lysosomes, where the cargo is degraded and the simple biochemical compounds are released for recycling or energy production. At the molecular level, autophagy is controlled by different functional complexes, which are required for the origin, elongation and maturation of the autophagosomes.<sup>3</sup> The hierarchical relationship among autophagic proteins allows a tight regulation of the process. At the initial step, the inductive complexes containing the serine/threonine kinase ULK1/Atg1 (unc-51 like autophagy activating kinase 1) and the class III phosphatidylinositol 3 -kinase (PtdIns3K) PIK3C3/Vps34 (phosphatidylinositol 3-kinase, catalytic subunit type 3/vacuolar protein sorting 34) are recruited to specific sites of the endoplasmic reticulum and provide a platform for autophagosome biogenesis, the so called omegasome.<sup>4</sup> The activity of the PtdIns3K generates a PtdIns3P-enriched region to which the complex formed by Atg2 and WIPI/Atg18 (WD repeat domain, phosphoinoside interacting) is recruited. Later, the ATG12–ATG5–ATG16L1 complex and the lipidation of LC3/Atg8 (microtubule-associated protein 1 light chain 3) to the emerging membrane allow the elongation of the phagophore.<sup>5</sup>

A number of studies in *Dictyostelium* have revealed the similarities, both morphological and molecular, of its autophagic process with that of animal cells.<sup>6</sup> In addition, this organism possesses several autophagic proteins that are conserved in mammals but absent in *S. cerevisiae* such as ATG101 and VMP1.<sup>2,6,7</sup> *Dictyostelium* mutant strains lacking Atg proteins display deficient autophagy and developmental abnormalities.<sup>8-11</sup> The most common phenotype is the block of development at the mound stage and the formation of multiple tips instead of normal fruiting bodies. This feature can be used as a screening parameter that might help to identify new genes involved in autophagy. Four multitipped mutants were described in the laboratory of William F. Loomis in 1999 and the proteins affected are named TipA, TipB, TipC, and

TipD (DictyBase Gene IDs: DDB\_G0281561, DDB\_G0276333, DDB\_G0267422, DDB\_G0275323).<sup>12, 13</sup> The 4 *tip* genes are expressed during vegetative growth and throughout development and have parallel but yet unknown functions during *Dictyostelium* development.<sup>13</sup> Sequence analysis reveals that *tipC* codes for a protein highly similar to the conserved VPS13 family. In humans, a member of this family, VPS13A, is the protein mutated in chorea-acanthocytosis.

Chorea-acanthocytosis (ChAc) (OMIM ID: 200150) is a rare autosomal recessive neurodegenerative disease. The most relevant symptoms are involuntary tensing of muscles (especially those in the face, mouth and limbs), neurodegeneration, and erythrocyte acanthocytosis.<sup>14-16</sup> This disorder is caused by the loss of function of the 360-kDa protein VPS13A (also known as Chorein), which is nearly absent in patients.<sup>17-21</sup> A mouse model of the disease has been reported.<sup>22</sup> It shows similarities to the human syndrome, such as brain pathology and red blood acanthocytosis, but displays a mild phenotype with late old-age onset.<sup>22</sup> In humans, VPS13A is expressed in a wide variety of tissues.<sup>23</sup> Defects in actin cytoskeleton regulation have been described in erythrocytes, platelets and vascular endothelial cells in the absence of VPS13A.<sup>24, 25</sup> In simpler organisms, null mutants in *Saccharomyces cerevisiae* and *Tetrahymena thermophila* suggest a role of Vps13 and VPS13A in membrane traffic and phagocytosis respectively but the precise VPS13 function is largely unknown.<sup>26-28</sup>

Here we describe that the VPS13-related protein TipC is required for efficient autophagy in *D. discoideum*. We extended our observations to human VPS13A by analyzing autophagy in RNA-interfered HeLa cells. Our results confirmed the role of VPS13A in autophagy and suggest the possibility that autophagy is involved in the etiology of chorea-acanthocytosis as described previously for other neurodegenerative diseases such as Parkinson, Alzheimer, and Huntington diseases.<sup>29</sup> This is relevant because, at present, no effective therapy for chorea-acanthocytosis is available and there is a growing interest of medical research in modulating autophagy as a therapeutic treatment.<sup>29-31</sup>

## Results

### Screening for autophagy defects in *Dictyostelium* multitipped mutants

*Dictyostelium* strains carrying gene disruptions in *tipA*, *tipB*, *tipC*, or *tipD* showed a similar phenotype in which large mounds split up to form multiple tips.<sup>13</sup> The similarity of this phenotype to the one observed in autophagy-deficient strains<sup>2</sup> led us to analyze autophagy in these mutants. To this end, autophagic flux was measured by a proteolytic cleavage assay described previously.<sup>32</sup> A large decrease in autophagic flux was detected in *tipC*<sup>-</sup> and *tipD*<sup>-</sup> strains (**Fig. 1A**) while *tipA*<sup>-</sup> and *tipB*<sup>-</sup> mutants showed similar levels than those of the wild type (**Fig. 1B**).

Analysis of the predicted protein sequences indicates that *tipD* (accession number EAL69727.1) codes for a protein similar to the yeast Atg16 and human ATG16L1. Of interest, the similarity of TipD to the homologous human protein is much higher (E-value: 2.2e-59) than to the yeast protein (E-value: 3.8e-4; E-values calculated with the LALIGN program from Biology WorkBench, <http://workbench.sdsc.edu/>) and the sequence also contains a large conserved WD-repeat region at the C terminus that is present in the human protein but absent in the yeast ortholog (**Fig. S1**). This domain might be involved in protein-protein interactions that have been conserved during evolution between *Dictyostelium* and mammalian cells. The identification of the *Dictyostelium* Atg16 ortholog and the confirmation of its role in autophagy validate our approach for the screening of new autophagic proteins using the multitipped phenotypic feature.

*tipC* (EAL73163.1) encodes a large protein of 3848 amino acids highly similar to the VPS13 family of proteins (**Fig. S2**). The human VPS13 family has 4 members (VPS13A/B/C/D) and TipC shows the highest homology with VPS13A and VPS13C (**Fig. S3**). No previous connection with autophagy has been reported for any of these proteins. Since mutations in human VPS13A leads to chorea-acanthocytosis, a rare disease that causes neurodegeneration, we focused on the study of *Dictyostelium* TipC and human VPS13A.

### The conserved C terminus of TipC is able to function independently to largely complement the mutant phenotype

TipC and VPS13A show 3 conserved regions at the N terminus and C terminus (**Fig. 2A to C**). Interestingly, the C terminus contains a small sequence similar to the C-terminal region of Atg2, as detected by the NCBI Conserved Domain Search using the Pfam database v27.0 (**Fig 2A and C**). This motif is depicted as ATG\_C-terminal domain and it is detected in both *Dictyostelium* TipC and human VPS13A with a significant E-value (2.42e-6 and 2.59e-6 respectively). The same region is detected in the yeast protein, but with a much less significant score (E-value: 0.29). The C-terminal region also contains a conserved domain of unknown function DUF1162. In order to assess the functionality of the Tip C-terminal region, we cloned and expressed the coding sequence fused to GFP in the *tipC*<sup>-</sup> mutant strain. The expression of the C-terminal polypeptide was confirmed by western blot using an anti-GFP antibody (**Fig. 2D**) and by confocal analysis of GFP fluorescence, that showed a cytoplasmic localization (**Fig. 2E**). Remarkably, the expression of the fragment largely complemented the mutant developmental phenotype (**Fig. 2F**). The complemented strain no longer displayed the characteristic multitipped phenotype. It succeeded to pass the mound stage and form normal-looking fruiting bodies. Calcofluor staining, that labels the cellulose walls of stalk and spore cells, showed that the few stalks present in the original mutant were abnormal. The complemented strain, however, showed fairly differentiated stalks (**Fig. 2G**). Nevertheless, the recovery was not complete because some of the structures were smaller and had thick stalks. Spore differentiation was also complemented according to the ellipsoid morphology of spores that were stained with calcofluor (**Fig. 2G**) and the number and viability of the formed spores. Spore efficiency was quantified in comparison with the wild-type AX4 strain and it recovered from  $1.70 \pm 0.03$  % in the original mutant to  $56.94 \pm 0.20$  % in the complemented strain. All together, the full length protein must be required for a total recovery, but the C-terminal region can function independently to some extent during development progression and stalk differentiation. Autophagy is required for these processes, and thus, the conserved C terminus of TipC probably has a critical function in autophagy.

Since autophagy and phagocytosis have been described to be connected<sup>33,34</sup> and *Tetrahymena thermophila* VPS13A is required for efficient phagocytosis,<sup>27</sup> we have also analyzed this process in the AX4, *tipC*<sup>-</sup> and the complemented strains. The results indicated a modest defect in phagocytosis in the mutant that was clearly recovered in the complemented strain (**Fig. 2H**).

### TipC and TipD regulate autophagy at different stages of autophagosome formation

To further characterize the role of TipC and TipD in autophagy and to determine which stage of autophagosome formation is affected, we expressed the autophagic markers GFP-Atg8 and GFP-Atg18 in *tipC*<sup>-</sup> and *tipD*<sup>-</sup> strains and visualized them by confocal microscopy. The number and the pattern of GFP-Atg8 puncta were altered in both strains. *tipC*<sup>-</sup> cells showed a reduced number of puncta and also some abnormally large structures absent in the wild-type strain. In the case of *tipD*<sup>-</sup> cells, they showed a much higher number of large structures, which appeared to be protein aggregates (**Fig. 3A**). GFP-Atg8 is an aggregate-prone marker and previous studies in *Dictyostelium* have shown a similar pattern in mutants of the autophagic proteins Atg1, Atg7 and Vmp1,<sup>7, 10</sup> with the presence of large ubiquitinated protein aggregates containing GFP-Atg8. Therefore, we analyzed the presence of ubiquitin-positive aggregates by immunofluorescence. Both mutant strains contained ubiquitinated aggregates although they were larger in *tipD*<sup>-</sup> cells, where the colocalization with GFP-Atg8 was also more evident and demonstrates that these large structures are not real autophagosomes (**Fig. 3B**). These abnormal patterns and the presence of ubiquitinated aggregates are consistent with the observed block in autophagy flux.

Due to the GFP-Atg8 tendency to aggregate, we used another marker, GFP-Atg18, for quantification analysis of puncta (**Fig. 4A and B**). GFP-Atg18 labels the initial stages of autophagosome formation and the puncta pattern is thinner than that of the GFP-Atg8. *tipC*<sup>-</sup> and *tipD*<sup>-</sup> cells showed a distinct GFP-Atg18 pattern. Puncta were accumulated in *tipD*<sup>-</sup> cells under growth and starvation conditions compared with the wild type. Since GFP-Atg18 is recruited to PtdIns3P-enriched endoplasmic reticulum-derived omegasomes,<sup>35</sup> this accumulation suggests that autophagosome formation is impaired at a stage posterior to the PtdIns3P signaling. This is consistent with the described role of Atg16 in the stage of autophagosome membrane elongation, downstream of Atg1 and PtdIns3K in the functional hierarchy.<sup>5</sup> Conversely, *tipC*<sup>-</sup> cells showed a significantly reduced number of GFP-Atg18 puncta. This is in agreement with an early blockade in autophagy, as observed in other *Dictyostelium* mutants lacking components that participate at the initial inductive signaling, such as the null mutant in Atg1.<sup>7</sup>



## **VPS13A depletion in human HeLa cells alters the pattern of autophagosome markers**

We next studied the consequences of VPS13A depletion in human HeLa cells in order to determine if the role in autophagy is conserved. Cells were transfected with control or *VPS13A* siRNAs and the GFP-LC3 and GFP-WIP1 pattern were observed in growth and starvation. Inhibition of *VPS13A* expression was determined by qRT-PCR. The *VPS13A* mRNA levels were reduced by  $89.5 \pm 2.9\%$  compared to the levels in control-transfected cells. Depletion of VPS13A protein was also determined by western blot (**Fig. 5A**). In HeLa cells stably expressing GFP-LC3, a high proportion of VPS13A-depleted cells showed an accumulation of puncta at the perinuclear region regardless of the nutritional conditions. In starvation, besides the perinuclear accumulation, the *VPS13A* siRNA-treated cells showed less translocation of the marker from the nucleus to the cytoplasm as compared with the control-transfected cells (**Fig. 5B**). Puncta quantification shows that *VPS13A*-silenced cells had an increase of puncta in growth and this number did not increase during starvation as did occur in the control cells (**Fig. 5C**). In HeLa *VPS13A*-depleted cells transiently transfected with the GFP-WIP1 marker, there were more GFP-WIP1 puncta than in control cells in both conditions, and there was not a significant increase following starvation (**Fig. 5D and E**). These results suggest that the accumulation of puncta might be the result of a deficiency in autophagic flux.

## **VPS13A is required for autophagic flux**

In order to analyze autophagic flux, siRNA-treated HeLa cells stably expressing GFP-LC3 were incubated in complete or starvation medium in the presence or absence of the lysosome inhibitor chloroquine. Protein extracts of at least 3 independent experiments were analyzed by western blot to detect GFP-LC3, cleaved GFP, and endogenous LC3-I/-II levels (**Fig. 6**). Since GFP-LC3 is degraded by autophagy, the level of GFP-LC3 has been previously shown to decrease during starvation.<sup>36-38</sup> As expected, this was the case for the control cells; however, high levels of the marker were present in the *VPS13A* siRNA-treated cells irrespective of the nutritional conditions (**Fig. 6A, B**). Another marker of autophagic flux is the cleaved GFP band, which is generated in part by autophagic degradation, as demonstrated by the GFP accumulation in chloroquine-treated cells. Once more, cleaved GFP accumulation was evident, together with a lesser

increase in the presence of chloroquine in starved *VPS13A*-depleted cells (**Fig. 6A and C**). These experiments indicate a lower autophagic flux during starvation.

The levels and turnover of endogenous LC3-I/-II were also quantified. Of note, the amount of LC3-I (the cytosolic form) in *VPS13A*-depleted cells was higher than in control cells, suggesting that conversion of LC3-I to LC3-II was affected (**Fig. 6A and D**). LC3 turnover was also consistent with a partial block of autophagic flux as the difference in the LC3-II levels between cells treated with or without chloroquine was reduced in *VPS13A*-silenced cells in both conditions (**Fig6. A and E**). All together, these results indicate that VPS13A is required for efficient autophagy at basal and starvation conditions in human HeLa cells.

## Discussion

We have characterized the role of TipC and TipD in *Dictyostelium* autophagy. TipD encodes a homolog of the *S. cerevisiae* Atg16 but shows a higher similarity to the human ATG16L1 because it contains a large C-terminal region that is not present in the yeast model. This is another example of the close similarity of the autophagy machinery between *Dictyostelium* and animal cells.<sup>2</sup>

*Dictyostelium* TipC and human VPS13A belong to the VPS13 family. To our knowledge, this is the first description of the role of this protein family in autophagy. *Dictyostelium* genome encodes other 5 Vps13 proteins, which have not been characterized yet. Similarly, the human genome also codes for several members of this family (VPS13A/B/C/D). Two of them, VPS13A and VPS13B, are responsible for the diseases chorea-acanthocytosis and Cohen syndrome, respectively. These diseases differ in many phenotypic and pathological aspects so it is likely that these proteins have diverged in their function. In addition, the analysis of amino acid identity shows that VPS13A and VPS13C are more similar between them, while VPS13B is more distantly related. The *Dictyostelium* TipC shows higher similarity to human VPS13A and VPS13C than to VPS13B. Interestingly, the expression of the C-terminal region of TipC allows the strain to progress in development, pass the finger stage and form differentiated spores and stalks, a process dependent on autophagy. These results suggest that the C-terminal region is important for autophagy regulation. This region contains 2 conserved domains also present in the human VPS13 proteins (DUF1162, and ATG\_C). The first one is a domain of unknown function, and the second one is a short region of similarity with Atg2, a protein that is recruited together with WIPI1/Atg18 to the sites of autophagosome formation.

The function of VPS13 proteins has been addressed in other model systems like the yeast *Saccharomyces cerevisiae* and the protozoa *Tetrahymena thermophila*. Interestingly, the *Tetrahymena* VPS13A localizes to the phagosome membrane and it is required for efficient phagocytosis.<sup>27</sup> A relation between autophagy and phagocytosis pathways has been described in mammalian phagocytes and this connection seems to be required for efficient killing and digestion of extracellular pathogens.<sup>34</sup> The phagocytosis defect observed in *Dictyostelium tipC* is not profound and could be due to a side effect of the autophagy blockade.

Yeast has only one Vps13 protein, which has been involved in membrane morphogenesis during sporulation but no defects in autophagy have been reported in the mutant strain so far. More specifically, the yeast *vps13Δ* cells show a depletion of PtdIns4P levels in prospore membranes.<sup>26, 39</sup> Distinct PtdIns-phosphates play essential roles in autophagy at different levels. For example, PtdIns(3,4,5)P<sub>3</sub> is essential for the signaling pathway that regulates TORC1 (TOR complex 1), and PtdIns(4,5)P<sub>2</sub> is required for the formation of autophagosomes originated from the plasma membrane.<sup>40</sup> Another important PtdIns molecule is PtdIns3P, which is formed at the ER-derived omegasome by the action of the class III PtdIns3K/Vps34. This signaling lipid is required for the recruitment of Atg18 and Atg2 to the phagophore site. Our results in *Dictyostelium* show a lower recruitment of the marker GFP-Atg18 in cells lacking TipC, which might indicate a defect at the level of PtdIns3P signaling. However, *VPS13A*-depleted HeLa cells, although impaired in autophagy flux, show the accumulation of autophagic markers, including WIPI1, the counterpart of Atg18. These results suggest that *Dictyostelium* TipC and human VPS13A regulate autophagy at different stages. Due to the large number of members of the VPS13 family in *Dictyostelium* and humans, we can not be certain if the *Dictyostelium* TipC is the precise functional counterpart of human VPS13A. It is likely that the different members could regulate autophagy at different levels or even distinct but related processes, an issue that will require the complete characterization of the different proteins of the family in both species.

Previous studies in human cells report that silencing *VPS13A* in K562-erythrocytic cells and vascular endothelial cells leads to changes in cell shape and cytoskeletal architecture.<sup>24, 25</sup> It has been suggested that *VPS13A*-depleted cells have lower activity of class I PI3K at the plasma membrane and this affects the control of actin cytoskeleton.<sup>25</sup> Class I PI3K inhibits autophagy through activation of TORC1, thus it is possible that *VPS13A*-depleted cells have a higher activation of the inductive stages of autophagy. However, even if this occurs, the concomitant accumulation of autophagic markers and the reduction in autophagic flux indicate that autophagosome maturation is impaired in *VPS13A*-silenced cells.

Malfunction of autophagy is associated with a variety of human diseases, including the most prominent neurodegenerative diseases,<sup>41</sup> and therefore, an increasing number of autophagy-modulating compounds are being tested in clinical trials.<sup>29</sup> The role of TipC and VPS13A in autophagy opens a new perspective in the functional

studies of this protein family and warrants further explorations on the involvement of autophagy in VPS13-related diseases, and more specifically, in chorea-acanthocytosis.

## Materials and Methods

***Dictyostelium* cell culture and genetic manipulations.** *Dictyostelium* Tip mutants were obtained from Dicty-stock center (kindly deposited by William F. Loomis). The parent strain, AX4, was used as wild type. Cells were grown axenically in complete medium (HL-5 or SIH medium; Formedium, HLB0102; SIH0102), or in association with *Klebsiella planticola* on SM-agar plates. Transformations were carried out by electroporation as described previously.<sup>42</sup> For synchronous development, axenically growing cells were washed from culture media by centrifugation, resuspended in PDF buffer (20 mM KCl, 9 mM K<sub>2</sub>HPO<sub>4</sub>, 13 mM KH<sub>2</sub>PO<sub>4</sub>, 1 mM CaCl<sub>2</sub>, 1 mM MgSO<sub>4</sub>, pH 6.4) and deposited on nitrocellulose filters (Millipore, HABP04700). The C-terminal region of TipC was amplified by PCR from genomic DNA and cloned into the pCGFPCTAP vector (fused to GFP at the C terminus).

**Calcofluor staining, sporulation, and phagocytosis assays.** Calcofluor (Sigma, F3543) staining and sporulation assays were performed as described previously.<sup>43</sup> Sporulation efficiency was calculated taking into account the spore production and the viability of the formed spores and given as a percentage related to the result of wild-type AX4 strain. For the phagocytosis assay, vegetative growing cells were incubated with fluorescent latex beads (Fluoresbrite 1.0 Micron Microspheres; Polysciences, 18860) and treated as indicated previously.<sup>44</sup> The amount of internalized fluorescence was measured in a fluorimeter and corrected by protein concentration in each sample.

**HeLa cell culture and small interfering (siRNA) experiments.** HeLa cells stably expressing GFP-LC3 were kindly provided by Aviva M Tolkovsky (John Van Geest Center for Brain Repair, Cambridge, UK) and described previously.<sup>45</sup> Cells were maintained in complete medium (DMEM, Dulbecco modified Eagle medium). Knockdown was performed by transfection of *VPS13A* siRNA (Ambion, s23340) or control siRNA (Ambion, control#2) with Lipofectamine RNAiMAX (Invitrogen, 13778-150), according to the manufacturer's instructions. Cells were transfected again with the same siRNAs after 2 days from the first transfection and the assays were carried out 3 days later. The level of depletion of *VPS13A* mRNA was measured by TaqMan PCR (Applied Biosystems, Hs00362891\_m1) and found to be  $89.5 \pm 2.9$  % for

all the experiments shown. GFP-WIPI-1 transfections were performed using Lipofectamine 2000 (Invitrogen, 11668-019) according to manufacturer's instructions and the plasmid pMX-IP GFP-WIPI-1 (Addgene, 38272).

**Autophagy detection in *Dictyostelium*.** *In vivo* confocal analysis of autophagic markers GFP-Atg8 and GFP-Atg18, immunofluorescence of ubiquitin aggregates, and proteolytic cleavage assay were performed as described previously.<sup>10, 32, 46</sup> For starvation assays, complete medium was replaced with PDF buffer or SIH medium without arginine and lysine (Formedium, SIH1001) 1 h prior to visualization.

**Autophagy detection in HeLa cells.** For confocal visualization, cells were incubated in complete medium (DMEM, Dulbecco modified Eagle medium) or starvation medium (EBSS, Earle balanced salt solution) for 2 h, fixed with 4% paraformaldehyde and mount with ProLongGold (Invitrogen, P36934) for visualization. For western blot analysis, total cell lysates were isolated using RIPA buffer from cells incubated in complete or starvation medium for 4 h in the presence or absence of 5  $\mu$ M chloroquine.

**Western blot and confocal microscopy.** Immunoblots were performed using anti-GFP (Sigma-Aldrich, G1544), anti-LC3B (Cell Signaling Technology, 2775), anti-GAPDH (Enzo LifeSciences, ADI-CSA-335) and anti-VPS13A (Santa Cruz Biotechnology, sc-109138) antibodies and the appropriate HRP-conjugated secondary antibody (Santa Cruz Biotechnology, sc-2004; sc2005). VPS13A detection was performed as previously described.<sup>21</sup> The western blot bands were quantified by densitometry (ImageJ software). Confocal images were acquired using an inverted Zeiss LSM 710 laser-scanning microscope (Carl-Zeiss-Strasse 22, 73447 Oberkochen, Germany). Puncta were counted using ImageJ software.

**Statistical analysis.** Data were shown as mean with SD (standard deviation) and analyzed using the Student t test. A *P* value <0.05, *P*<0.01 or *P*<0.001 was denoted by \*, \*\*, or \*\*\*, respectively.



## Acknowledgements

Sequence data for *Dictyostelium* were obtained from the Genome Sequencing Centers of the University of Cologne, Germany; the Institute of Molecular Biotechnology, Department of Genome Analysis, Jena; the Baylor College of Medicine in Houston, Texas, USA; and the Sanger Center in Hinxton, Cambridge, United Kingdom. Tip-deficient strains were obtained from Dicty Stock Center and deposited by William F. Loomis. We thank Patricia Boya and Aviva Tolkovsky for providing the HeLa cells stably expressing GFP-LC3 and M. J. Obregón for providing the quantitative PCR instrument. This work was supported by grants BFU2009-09050 and BFU2012-32536 from the Spanish Ministerio de Ciencia e Innovación. We also thank the help of Obra Social Caja de Burgos para Jóvenes Excelentes. SMB is recipient of a predoctoral fellowship from Universidad Autónoma de Madrid.

## References

1. Yang Z, Klionsky DJ. Mammalian autophagy: core molecular machinery and signaling regulation. *Current opinion in cell biology* 2010; 22:124-31.
2. Calvo-Garrido J, Carilla-Latorre S, Kubohara Y, Santos-Rodrigo N, Mesquita A, Soldati T, et al. Autophagy in *Dictyostelium*: genes and pathways, cell death and infection. *Autophagy* 2010; 6:686-701.
3. Mizushima N, Yoshimori T, Ohsumi Y. The role of Atg proteins in autophagosome formation. *Annual review of cell and developmental biology* 2011; 27:107-32.
4. Axe EL, Walker SA, Manifava M, Chandra P, Roderick HL, Habermann A, et al. Autophagosome formation from membrane compartments enriched in phosphatidylinositol 3-phosphate and dynamically connected to the endoplasmic reticulum. *J Cell Biol* 2008; 182:685-701.
5. Itakura E, Mizushima N. Characterization of autophagosome formation site by a hierarchical analysis of mammalian Atg proteins. *Autophagy* 2010; 6:764-76.
6. King JS. Autophagy across the eukaryotes: Is *S. cerevisiae* the odd one out? *Autophagy* 2012; 8:1159-62.
7. King JS, Veltman DM, Insall RH. The induction of autophagy by mechanical stress. *Autophagy* 2011; 7:1490-9.
8. Otto GP, Wu MY, Kazgan N, Anderson OR, Kessin RH. Macroautophagy is required for multicellular development of the social amoeba *Dictyostelium discoideum*. *J Biol Chem* 2003; 278:17636-45.
9. Otto GP, Wu MY, Kazgan N, Anderson OR, Kessin RH. *Dictyostelium* macroautophagy mutants vary in the severity of their developmental defects. *J Biol Chem* 2004; 279:15621-9.
10. Calvo-Garrido J, Escalante R. Autophagy dysfunction and ubiquitin-positive protein aggregates in *Dictyostelium* cells lacking Vmp1. *Autophagy* 2010; 6:100-9.
11. Tung SM, Unal C, Ley A, Pena C, Tunggal B, Noegel AA, et al. Loss of *Dictyostelium* ATG9 results in a pleiotropic phenotype affecting growth, development, phagocytosis and clearance and replication of *Legionella pneumophila*. *Cellular microbiology* 2010; 12:765-80.
12. Stege JT, Shaulsky G, Loomis WF. Sorting of the initial cell types in *Dictyostelium* is dependent on the tipA gene. *Dev Biol* 1997; 185:34-41.
13. Stege JT, Laub MT, Loomis WF. tip genes act in parallel pathways of early *Dictyostelium* development. *Dev Genet* 1999; 25:64-77.
14. Dobson-Stone C, Rampoldi L, Bader B, Velayos Baeza A, Walker RH, Danek A, et al. Chorea-Acanthocytosis. In: Pagon RA, Bird TD, Dolan CR, Stephens K, Adam MP, eds. *GeneReviews*. Seattle (WA), 1993.
15. Walterfang M, Looi JC, Styner M, Walker RH, Danek A, Niethammer M, et al. Shape alterations in the striatum in chorea-acanthocytosis. *Psychiatry Res* 2011; 192:29-36.
16. Neutel D, Miltenberger-Miltenyi G, Silva I, de Carvalho M. Chorea-acanthocytosis presenting as motor neuron disease. *Muscle & nerve* 2012; 45:293-5.
17. Ueno S, Maruki Y, Nakamura M, Tomemori Y, Kamae K, Tanabe H, et al. The gene encoding a newly discovered protein, chorein, is mutated in chorea-acanthocytosis. *Nature genetics* 2001; 28:121-2.

18. Dobson-Stone C, Danek A, Rampoldi L, Hardie RJ, Chalmers RM, Wood NW, et al. Mutational spectrum of the CHAC gene in patients with chorea-acanthocytosis. *European journal of human genetics* : EJHG 2002; 10:773-81.
19. Velayos-Baeza A, Vettori A, Copley RR, Dobson-Stone C, Monaco AP. Analysis of the human VPS13 gene family. *Genomics* 2004; 84:536-49.
20. Tomiyasu A, Nakamura M, Ichiba M, Ueno S, Saiki S, Morimoto M, et al. Novel pathogenic mutations and copy number variations in the VPS13A gene in patients with chorea-acanthocytosis. *Am J Med Genet B Neuropsychiatr Genet* 2011; 156B:620-31.
21. Dobson-Stone C, Velayos-Baeza A, Filippone LA, Westbury S, Storch A, Erdmann T, et al. Chorein detection for the diagnosis of chorea-acanthocytosis. *Annals of neurology* 2004; 56:299-302.
22. Tomemori Y, Ichiba M, Kusumoto A, Mizuno E, Sato D, Muroya S, et al. A gene-targeted mouse model for chorea-acanthocytosis. *Journal of neurochemistry* 2005; 92:759-66.
23. Kurano Y, Nakamura M, Ichiba M, Matsuda M, Mizuno E, Kato M, et al. In vivo distribution and localization of chorein. *Biochemical and biophysical research communications* 2007; 353:431-5.
24. Alesutan I, Seifert J, Pakladok T, Rheinlaender J, Lebedeva A, Towhid ST, et al. Chorein Sensitivity of Actin Polymerization, Cell Shape and Mechanical Stiffness of Vascular Endothelial Cells. *Cell Physiol Biochem* 2013; 32:728-42.
25. Foller M, Hermann A, Gu S, Alesutan I, Qadri SM, Borst O, et al. Chorein-sensitive polymerization of cortical actin and suicidal cell death in chorea-acanthocytosis. *FASEB journal : official publication of the Federation of American Societies for Experimental Biology* 2012; 26:1526-34.
26. Park JS, Neiman AM. VPS13 regulates membrane morphogenesis during sporulation in *Saccharomyces cerevisiae*. *Journal of cell science* 2012; 125:3004-11.
27. Samaranayake HS, Cowan AE, Klobutcher LA. Vacuolar protein sorting protein 13A, TtVPS13A, localizes to the tetrahymena thermophila phagosome membrane and is required for efficient phagocytosis. *Eukaryotic cell* 2011; 10:1207-18.
28. Brickner JH, Fuller RS. SOI1 encodes a novel, conserved protein that promotes TGN-endosomal cycling of Kex2p and other membrane proteins by modulating the function of two TGN localization signals. *The Journal of cell biology* 1997; 139:23-36.
29. Jiang P, Mizushima N. Autophagy and human diseases. *Cell research* 2014; 24:69-79.
30. Yang ZJ, Chee CE, Huang S, Sinicrope F. Autophagy modulation for cancer therapy. *Cancer biology & therapy* 2011; 11:169-76.
31. Xie M, Morales CR, Lavandero S, Hill JA. Tuning flux: autophagy as a target of heart disease therapy. *Curr Opin Cardiol* 2011; 26:216-22.
32. Calvo-Garrido J, Carilla-Latorre S, Mesquita A, Escalante R. A proteolytic cleavage assay to monitor autophagy in *Dictyostelium discoideum*. *Autophagy* 2011; 7:1063-8.
33. Shui W, Sheu L, Liu J, Smart B, Petzold CJ, Hsieh TY, et al. Membrane proteomics of phagosomes suggests a connection to autophagy. *Proc Natl Acad Sci U S A* 2008; 105:16952-7.
34. Mehta P, Henault J, Kolbeck R, Sanjuan MA. Noncanonical autophagy: one small step for LC3, one giant leap for immunity. *Current opinion in immunology* 2014; 26:69-75.

35. Polson HE, de Lartigue J, Rigden DJ, Reedijk M, Urbe S, Clague MJ, et al. Mammalian Atg18 (WIPI2) localizes to omegasome-anchored phagophores and positively regulates LC3 lipidation. *Autophagy* 2010; 6:506-22.
36. Dorsey FC, Steeves MA, Prater SM, Schroter T, Cleveland JL. Monitoring the autophagy pathway in cancer. *Methods in enzymology* 2009; 453:251-71.
37. Klionsky DJ, Abdalla FC, Abeliovich H, Abraham RT, Acevedo-Arozena A, Adeli K, et al. Guidelines for the use and interpretation of assays for monitoring autophagy. *Autophagy* 2012; 8:445-544.
38. Ni HM, Bockus A, Wozniak AL, Jones K, Weinman S, Yin XM, et al. Dissecting the dynamic turnover of GFP-LC3 in the autolysosome. *Autophagy* 2011; 7:188-204.
39. Park JS, Okumura Y, Tachikawa H, Neiman AM. SPO71 encodes a developmental stage-specific partner for VPS13 in *Saccharomyces cerevisiae*. *Eukaryotic cell* 2013.
40. Dall'armi C, Devereaux KA, Di Paolo G. The role of lipids in the control of autophagy. *Current biology : CB* 2013; 23:R33-45.
41. Schneider JL, Cuervo AM. Autophagy and human disease: emerging themes. *Current opinion in genetics & development* 2014; 26C:16-23.
42. Pang KM, Lynes MA, Knecht DA. Variables controlling the expression level of exogenous genes in *Dictyostelium*. *Plasmid* 1999; 41:187-97.
43. Escalante R, Sastre L. A serum response factor homolog is required for spore differentiation in *Dictyostelium*. *Development* 1998; 125:3801-8.
44. Rivero F, Maniak M. Quantitative and microscopic methods for studying the endocytic pathway. *Methods in molecular biology* (Clifton, NJ 2006; 346:423-38.
45. Bampton ET, Goemans CG, Niranjana D, Mizushima N, Tolkovsky AM. The dynamics of autophagy visualized in live cells: from autophagosome formation to fusion with endo/lysosomes. *Autophagy* 2005; 1:23-36.
46. Mesquita A, Calvo-Garrido J, Carilla-Latorre S, Escalante R. Monitoring autophagy in *Dictyostelium*. *Methods in Molecular Biology* 2013; 983:461-70.

## Figure legends

**Figure 1.** Autophagic flux is decreased in *tipC*<sup>-</sup> and *tipD*<sup>-</sup> cells. Proteolytic cleavage assay was performed in strains transfected with the marker GFP-Tkt-1. Protein extracts were analyzed by western blot using anti-GFP antibody. **(A)** The accumulation of cleaved GFP fragment (black arrows) in the presence of 100 mM NH<sub>4</sub>Cl is reduced in *tipC*<sup>-</sup> and *tipD*<sup>-</sup> mutants compared to the wild-type AX4 strain. **(B)** *tipA*<sup>-</sup> and *tipB*<sup>-</sup> levels of cleaved GFP are similar to those of AX4. The complete GFP-Tkt-1 fusion protein is marked by white arrows and the stars indicate nonspecific immunoreactive bands.

**Figure 2.** The conserved C terminus of TipC largely complements the *tipC*<sup>-</sup> phenotype. **(A)** Scheme of the 3848-amino acid TipC protein and the conserved domains (colored boxes). The line under the scheme depicts the fragment expressed in the complementation experiments. Alignment of the N-terminal **(B)** and C-terminal **(C)** regions of *D. discoideum* TipC (EAL73163.1) and the human VPS13A (NP\_150648.2) proteins using the ClustalW algorithm and shaded using the Boxshade tool at the SDSC Biology WorkBench server (<http://workbench.sdsc.edu/>). Identical residues are *shaded black*, and similar residues are *shaded gray*. Colored boxes frame the conserved domains. **(D)** Western blot using anti-GFP antibody confirmed the presence of a unique band of 150 kDa in the transformed strain with the C-terminal region of TipC (amino acids 2725 to 3848) fused to GFP. Lanes 1 and 3 correspond to protein extracts of AX4 and *tipC*<sup>-</sup> that do not express the fused proteins and were used as controls of antibody specificity. **(E)** The C-terminal TipC polypeptide fused to GFP is localized in the cytoplasm according to *in vivo* confocal microscopy visualization of transformed cells. **(F)** The complemented strain rescues fruiting body development. Scale bar: 100 μm. **(G)** Calcofluor staining shows details of stalk differentiation and spore shape of the different strains. For *tipC*<sup>-</sup> mainly cell debris could be visualized. Scale bar: 10 μm. Spore efficiency of each strain (sp. eff.) is indicated. **(H)** Phagocytosis rate of the wild-type, the mutant, and the complemented strain was measured through the internalized fluorescent signal of cells that were previously incubated with fluorescent beads during the indicated times.

**Figure 3.** The pattern of GFP-Atg8 is altered in *tipC*<sup>-</sup> and *tipD*<sup>-</sup> cells. **(A)** *In vivo* confocal analysis of cells expressing GFP-Atg8 in growing and starvation conditions. Puncta formation is inhibited in starved *tipC*<sup>-</sup> cells compared with AX4. In contrast, large aggregates of the autophagosome marker are evident in *tipD*<sup>-</sup> cells in both growing conditions. **(B)** Immunofluorescence of ubiquitin in the cells expressing GFP-Atg8 demonstrates the presence of ubiquitin-positive protein aggregates in both mutants. The ubiquitin structures are smaller in *tipC*<sup>-</sup> cells and do not always colocalize with GFP-Atg8, while the autophagosome marker is clearly contained in the large *tipD*<sup>-</sup> ubiquitinated aggregates. Scale bar: 10  $\mu$ m.

**Figure 4.** GFP-Atg18 puncta signaling is decreased in *tipC*<sup>-</sup> cells and accumulates in *tipD*<sup>-</sup> cells. **(A)** Cells expressing GFP-Atg18 were analyzed *in vivo* by confocal microscopy. Puncta formation is induced under starvation conditions in AX4 cells. However, most of *tipC*<sup>-</sup> cells do not display any puncta. Conversely, many puncta are observed *tipD*<sup>-</sup> cells regardless of the nutritional conditions. Scale bar: 10  $\mu$ m. **(B)** Quantification of GFP-Atg18 puncta of at least 100 cells in blinded images from 3 independent experiments. Results are shown as mean values with standard deviations of the percentage of cells showing the indicated number of puncta. Asterisks indicate the level of significance of the Student t test (\* < 0.05; \*\* < 0.01).

**Figure 5.** VPS13A downregulation causes GFP-LC3 and GFP-WIPI1 accumulation. **(A)** Western blot of control and *VPS13A* siRNA-transfected cells. A band of the VPS13A-predicted molecular weight decreases in the *VPS13A*-silenced cells. The asterisks indicate nonspecific immunoreactive bands. **(B and C)** HeLa cells stably expressing GFP-LC3 were transfected with control or *VPS13A* siRNAs and the pattern observed by confocal microscopy. *VPS13A*-depleted cells show accumulated puncta and less translocation from the nucleus to the cytoplasm during starvation. **(D and E)** HeLa cells were transfected with GFP-WIPI1 and the pattern observed by confocal microscopy. The number of puncta is higher in *VPS13A* siRNA-treated cells and does not significantly increase following starvation. The graphs show the mean and the standard deviation of puncta quantification of more than 40 cells from 3 independent experiments. Asterisks indicate the level of significance of the Student t test (\* < 0.05; \*\* < 0.01). Scale bar: 10  $\mu$ m.

**Figure 6.** A reduced autophagic flux is observed in *VPS13A* siRNA-treated cells. (A) GFP-LC3, free GFP, and endogenous LC3-I/-II were analyzed by western blot from control or *VPS13A* siRNA-treated cells under growth or starvation conditions with or without 5  $\mu$ M chloroquine (CQ). (B, C, D, E) Densitometric quantification showing the mean and the standard deviations of at least 3 independent experiments. The data was normalized against GAPDH. Asterisks indicate the level of significance of the Student t test (\* < 0.05; \*\* < 0.01; \*\*\* < 0.001).

Fig.1

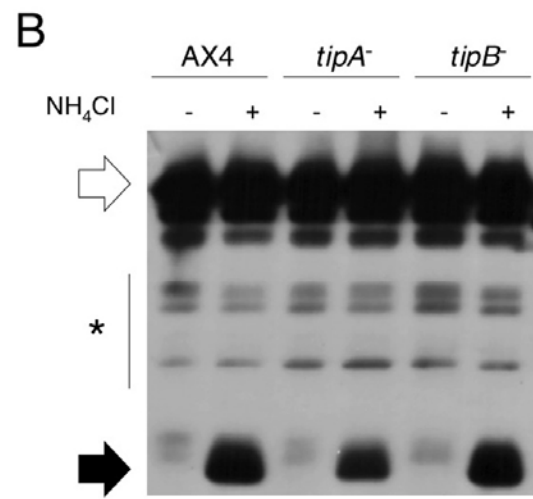
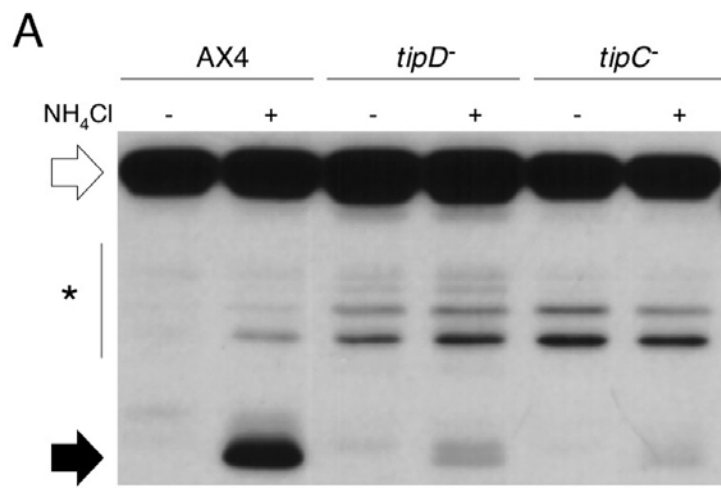




Fig.2

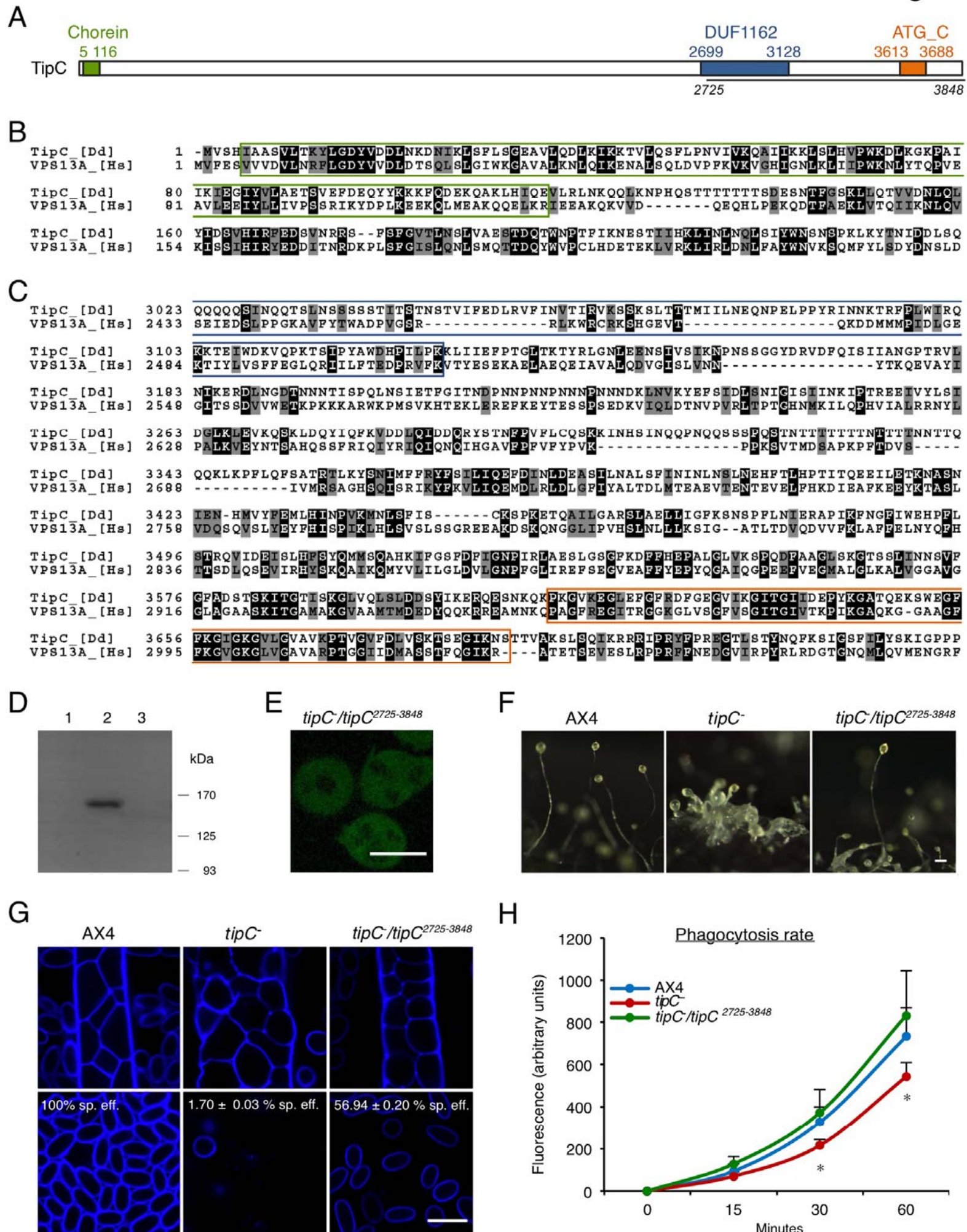


Fig.3

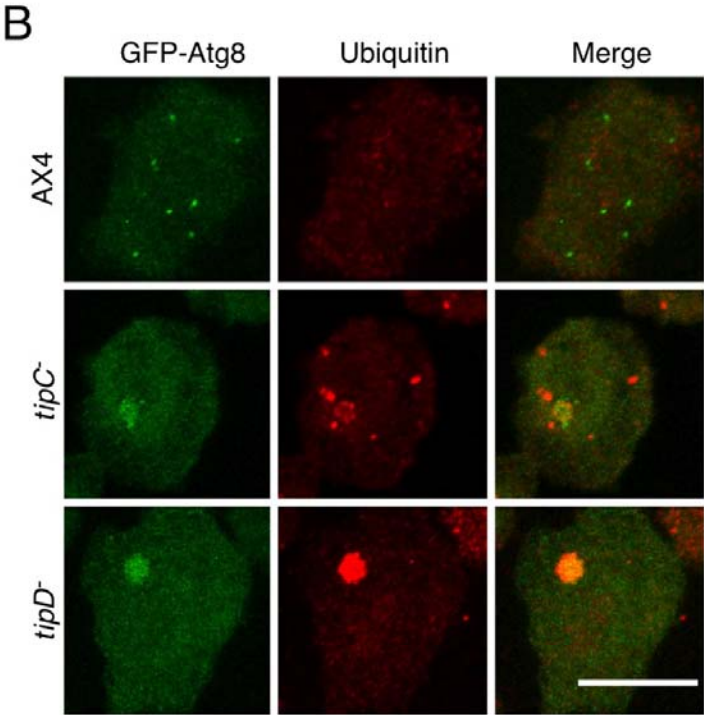
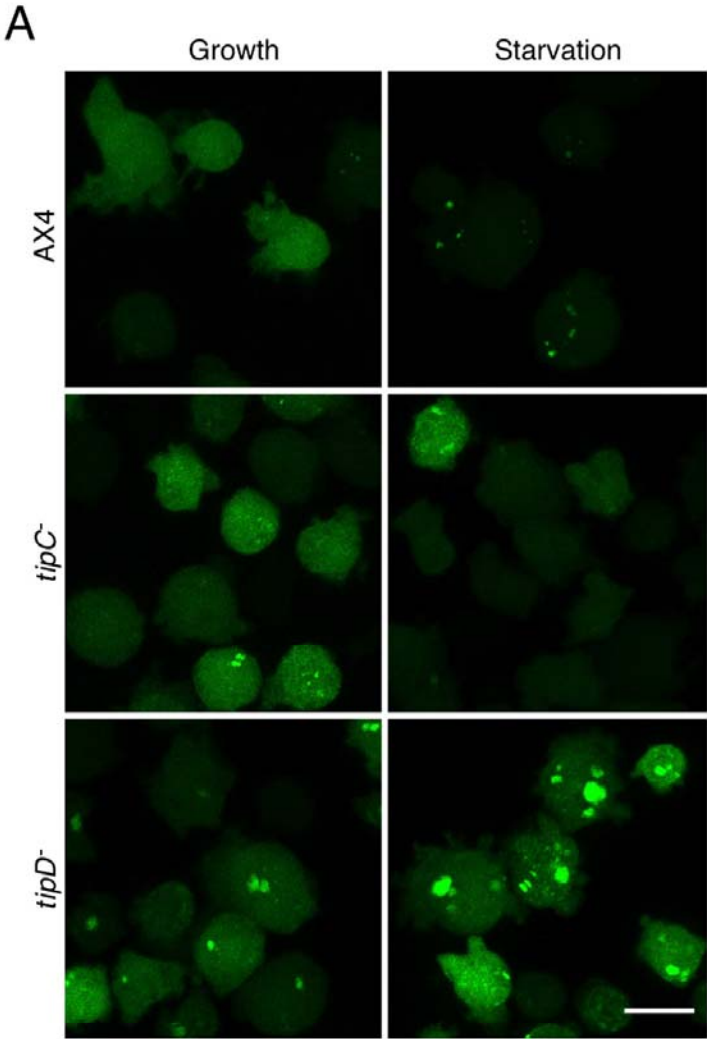


Fig.4

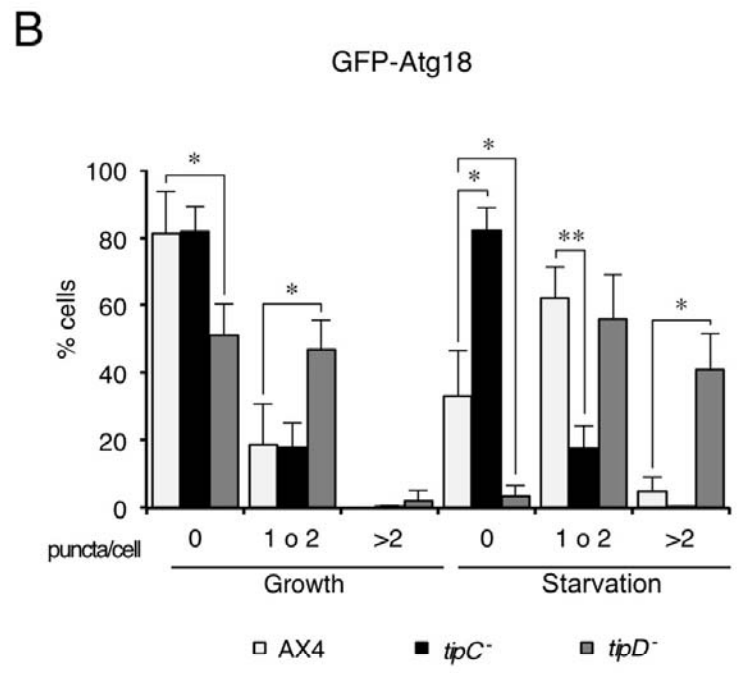
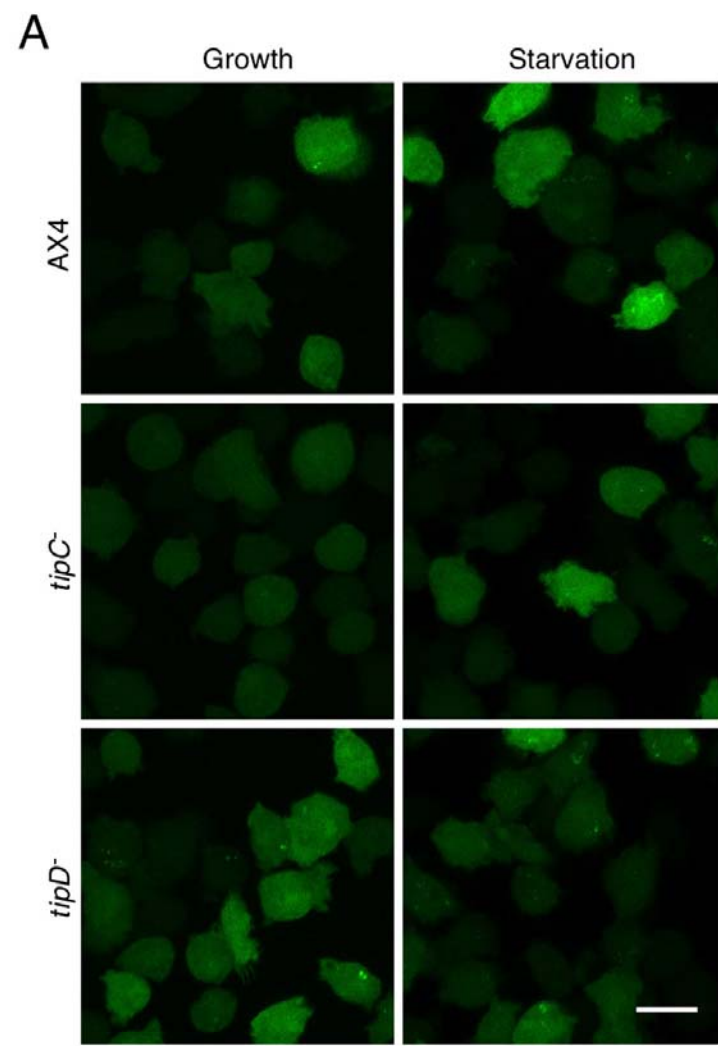




Fig.5

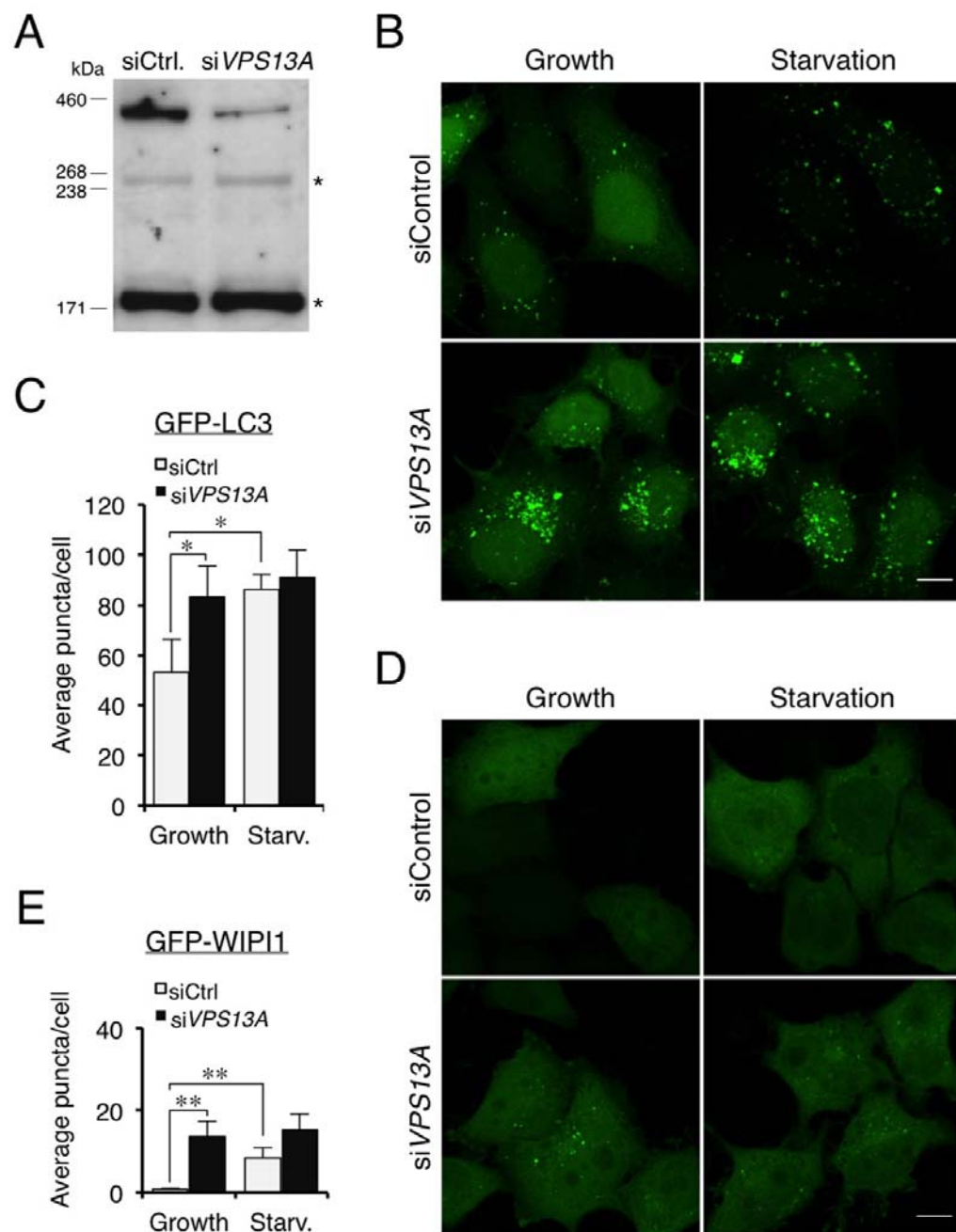
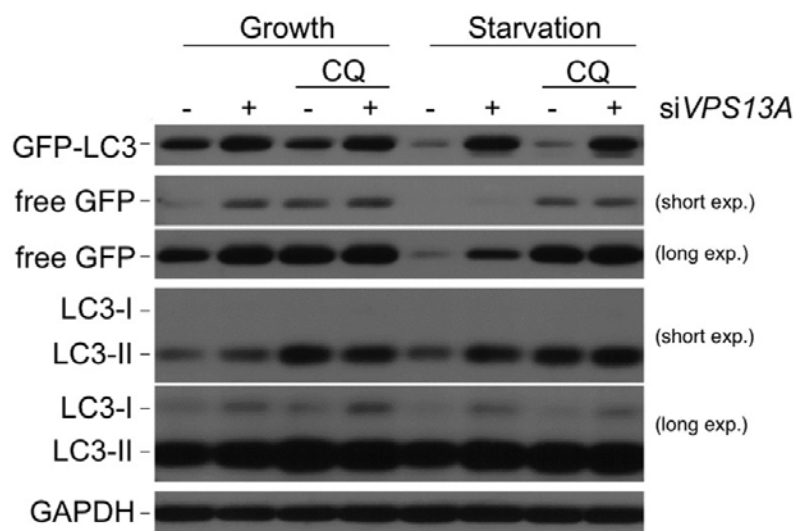
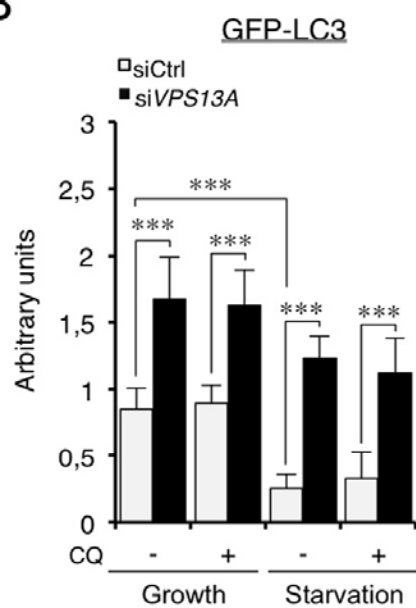


Fig.6

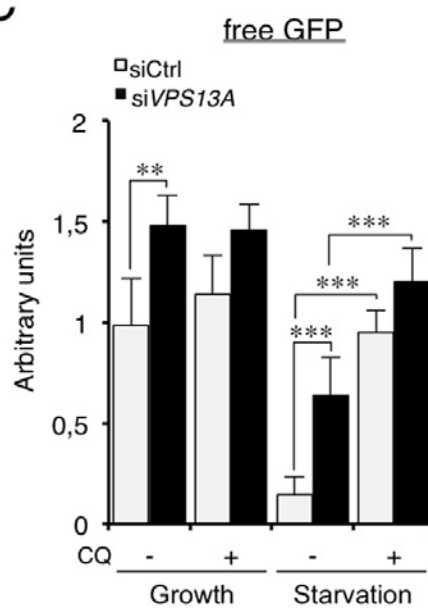
A



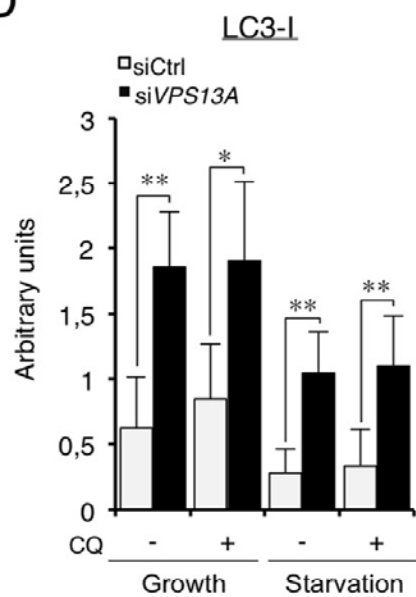
B



C



D



E

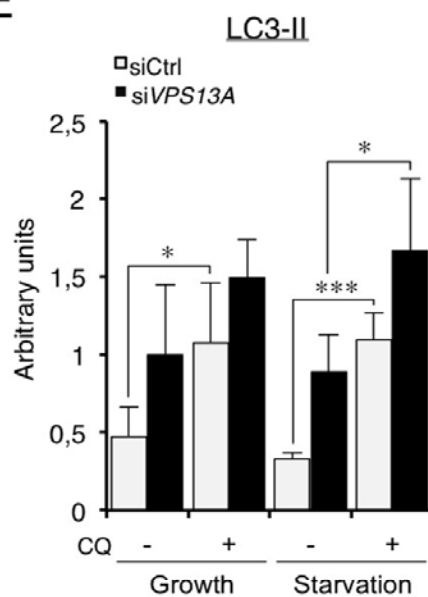
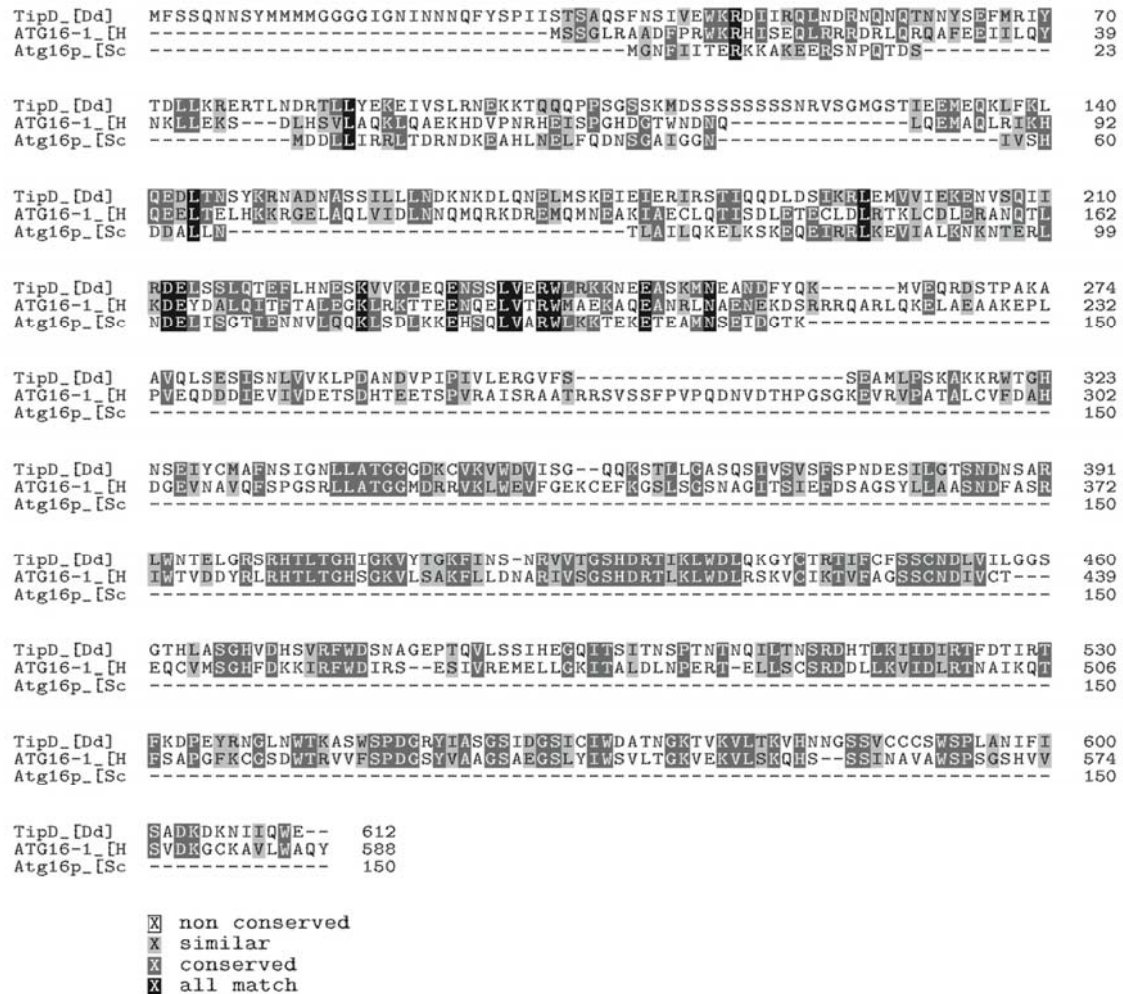


Fig. S1



**Figure S1.** Amino acid alignment of TipD, with *H. sapiens* ATG16L1 and *S. cerevisiae* Atg16. *Dictyostelium discoideum* TipD (EAL69727.1) was aligned with *H. sapiens* ATG16L1 (NP\_060444.3) and *S. cerevisiae* Atg16 (NP\_013882.1) using the ClustalW algorithm and shaded using the Textshade tool at the SDSC Biology WorkBench server (<http://workbench.sdsc.edu/>).

Fig. S2

A

TipC_[Dd]	-MVSHIAASVLTGYLGDYVDDLNKDNKISFLSGEAVLQDKIKKTVLQSFNPVIVKQAIKKLSLHVP	69
VPS13A_[Hs]	MVFESVVDVNLNRLGDDYVDDLTSLSLGIWKGAVALKNLQIKENALSQLDVPFVKVGHIGNLKLIIIP	70
VPS13C_[Hs]	MVLESVVDLLNRLGDDYVDDLTSLSLGIWKGAVALKNLQIKENALSQLDVPFVKVGHIGNLKLIIIP	70
Vps13_[Sc]	-MLESIAANLLNRLGDDYVDDLTSLSLGIWKGAVALKNLQIKENALSQLDVPFVKVGHIGNLKLIIIP	69
TtVPS13A_[	-MFGQLISSVLDKVAGEYVVLGLNKENLNIGFSGEVKIEVSLNPNVNNMLDLPIISHQYSIKKLEKVP	69
TipC_[Dd]	WRDITKGGKPAITIKTEGIYVVAETSVFDEQYKKKFQDEKQAKLHTQEVLRNLKQQLKNPHSTTTTTTTS	139
VPS13A_[Hs]	WKNLYTQPVAVLEIYLLIVPSSR-----TKYDPLKEEKQMEAKQQLKRIIEAKQVVVDQEQHL	132
VPS13C_[Hs]	WKNLYGEAVVATLEGLYLLVVPAS-----TKYDAVKEEKSLQDVKKELSRIEEALQAAEKDKPK	132
Vps13_[Sc]	WSSIKNKPVKIITDCYLLCSPRSEDHENEEMIKRAFRLKMRKVSEWELTNQARILSTQSENKTSSSSS	139
TtVPS13A_[	FKNIGSKPVVFLDGLYLVVTPKEQ-----KEWTFKDFKAFKNNKTNIESFAAECYSKIAAK--QQEKNK	132
TipC_[Dd]	DESN-TFGSKLLQTVVDNLQLYIDSVHIREF---SVNRRSFSFGVTLNSLVAESTDQTWTFIKNES-	204
VPS13A_[Hs]	PEKQDTFAEKLVTQIKNLQVKKISSIHIREF---DITNRDKELSEGLSLQNLMSQTTDQYVPCLHDETE-	200
VPS13C_[Hs]	EAKKDTFVEKLATQVIKNVQVKITDIHIREF---DVTDPKRELSEGLTLGELSLLANEHWTFCILNEAD-	200
Vps13_[Sc]	EKNNAAGFMQSLTTKIDNLQVTKINIHIREFMDGTFTTGESSVGLTLNELSAVSDSNWASFIITITQ-	208
TtVPS13A_[	VEKDAGYIQKLTMKIVDNLQITIRNHIREF---TITKYSKFCFLDKIETITNKDGIKTEVDRTAE	198
TipC_[Dd]	-----TIIHKLINLQSLIYWNSSPKLKY-----TNIDDLSQLKSMIKKEDSGKQQQQQQQQGEEQDD	265
VPS13A_[Hs]	-----KLVRKLIRLDNLFAYWNVKSQMFYL-----SDYDNLDDLNKNGIVNENI-----	244
VPS13C_[Hs]	-----KTIYKLIRDSLAYSWNVCSMSYQ-----RSREQLDQLKNEILTSGN-----	244
Vps13_[Sc]	-----NITHKLLTNSLCLYWNTPPIISDDQDRSLNLFVIRGFKDMIASKNS-----	257
TtVPS13A_[	ESKNEPMRKLVLVISNAGVYWMANETRLIS---DLAEPHKIRIENGMIQKCGQ-----	247
TipC_[Dd]	EIEEDYFLSTESRKQYIIDPISAKLKVIVINKSIIPSEVIPKYNLFEEFKTDISLSDYQYKDTITGILES	335
VPS13A_[Hs]	-----VPEGYDFVFRPISANAKLVNRRSDFDFSAPKINLEIELHNTAIEFNKPQVFSIMELLES	304
VPS13C_[Hs]	-----IPPNYQYIEQPISASAKLYMNPYAESELTKPKLDCNTEIQNTAIEETKPYLSMIDLLES	304
Vps13_[Sc]	-----TAPKHQYILKPVSLGKELISINKLG-STEEQPHIDLMFYDFEGLEDDTDLHLVLLS	316
TtVPS13A_[	-----AKTDEPVDFLEKISSQISLTNNK--GNFEVPEIKVNLNLEHTLHQQKQLQVIEQIEF	306

B

TipC_[Dd]	ILNALSEFININLSLN---EHFTLHPTITQEEILETKNASNIENHMVYFEMLHINPVKMNLSTFISCKSPK	3451
VPS13A_[Hs]	IYALTBLMTAEAVTEN--TEVELFHKDIEAFKEEYKTASLDQSQVSLYEFYHISPKLHLSSLSSGRE	2787
VPS13C_[Hs]	LGAITLALFTPTTDEAERRRKLIIQDIDALNAELMETSMTDMSILSFFEFHISPVKLHLSSLSSGGE	3303
Vps13_[Sc]	LYAMMDFIKFPSPWIMDSRDYKYDEETQLPDDVSLKTAGD-----IYFEIYFHQIDTDLHLVLLS	2762
TtVPS13A_[	ISTLLDFLKGVVEARYDADAQSINTLKEYLDETSQTEKNENIKFKWQECETPPTSPPTFINQLILSNIEI	3076
TipC_[Dd]	ETQAILG---ARSLAELLIGFKN-SFFLNTERAPIKENGFIWEHPFLSTRQVIDEISLHFSYQMMSSAH	3517
VPS13A_[Hs]	EAKDSKQNGGLIPVHSLNLLKLSIGATITDQDDVVFKAFFELNYQHHTISDQSEVIRHYSKQAIKQMY	2857
VPS13C_[Hs]	ESDKEKQE--MFAVHSLNLLKLSIGATITDQDDVVFKAFFELNYQHHTISDQSEVIRHYSKQAIKQMY	3371
Vps13_[Sc]	EISPLGAEEETESFSSSLYVHMFAMTLGNINEAPVKVNSLFMDNVRVPLPILMDHIERHYTTFQVYQIH	2832
TtVPS13A_[	ALTFAKVKTNDSLDNLVLSVFTALGVALADIEASLKLNGIKLVNCEETASGIVSKLTAHYKDAQISEVL	3146
TipC_[Dd]	KIFGSFFDIGNPIRLAESLSCGFKDFHEHPALCLVKS--PQDFAAGISKCTSSLINNSVFCFADSTSKIT	3585
VPS13A_[Hs]	VLLICLDVLCNPFGLIREFSECVAEAFYEPYQCAIQ--PEEFVECMALCLKALVGGAVCGLAGAASKIT	2925
VPS13C_[Hs]	VLLICLDVLCNPFGLIREFSECVAEAFYEPYQCAIQ--PEFAEGVLICVRSFGHTVGCAGAVSVRIT	3439
Vps13_[Sc]	KILGSAFCGNPVGLFNTISSGVWDLFYEPYQCYMMNDPQBIIGIHLAKGGLSFAKKTVGLSDSSMSKFT	2902
TtVPS13A_[	KALGSLNITGNPVGLFQNTISTGVTDLFTTPAEGFVKG--PLGGGLGIMQGASSLIKNIMAGAFNSVNKIT	3214
TipC_[Dd]	GTISKGLVQLSLDDSVIKERQESNKQKPKGVKEGLEFCFRDCEGVKICITGIDEPYKGTQEKSWECF	3655
VPS13A_[Hs]	CAMAKCVAMTMDYDQKRRBAMNKQPAFGREGITRCGKGLVSCFVSCITCIVTKPIKCAQKG-GAAGF	2994
VPS13C_[Hs]	CSVKGGLAATMDKEYQKRRBELSRQPRFGDSARGCGGLRGLVGGVTCIITKPVGAKKE-GAAGF	3508
Vps13_[Sc]	CSMAKGLS-VTQDLERQVRRL-LQRIKNNRNANSAQSFASTLGSCLSGIALDIPYRAMQKE-GAAGF	2969
TtVPS13A_[	GSLSSGISALCMDREYLREDRMRSKRPHLVGAVQGVTSIFSGVANGITGVFLKPFEGAKKG-GALGF	3283
TipC_[Dd]	FKGIGKGVLCYAVKPTVCVFDLVSKTSECIKNSTTAKSLSQIKRRRIIPRYEP-REGTLSTYNQFKSIGS	3724
VPS13A_[Hs]	FKGVCKGLVCYAVARPTCGIIDMASTTFQGIKRATE-TSEVESLRP---PRFEN-EDGVIRPYRLRDGTGN	3059
VPS13C_[Hs]	FKGIGKGVLCYAVARPTCGIIDMASTTFQGIQRAAESTEESVSLRP---PRLIH-EDGIIRPYDRQSECS	3574
Vps13_[Sc]	FKGIGKGVLCYAVARPTCGIIDMASTTFQGIQRAAESTEESVSLRP---PRLIH-EDGIIRPYDRQSECS	3037
TtVPS13A_[	LKGIGKGVLCYAVKPTVCVFDLVSKTSECIKNSTTAKSLSQIKRRRIIPRYEP-REGTLSTYNQFKSIGS	3353

**Figure S2.** Amino acid alignment of the N (A) and C terminus (B) of TipC with VPS13 proteins of other organisms. *Dictyostelium discoideum* TipC (EAL73163.1) was aligned with *H. sapiens* VPS13A (NP\_150648.2) and VPS13C (NP\_060154.3), *S. cerevisiae* Vps13 (CAA97491.1) and *Tetrahymena termophila* VPS13A (ADM47433.1) using the ClustalW algorithm and shaded using the Textshade tool at the SDSC Biology WorkBench server (<http://workbench.sdsc.edu/>).

Fig. S3

	TipC	VPS13A	VPS13B	VPS13C
<b>VPS13A</b>	19.6% (1.1e-78)	-	-	-
<b>VPS13B</b>	18.1% (1.5e-23)	18.1% (1.4e-17)	-	-
<b>VPS13C</b>	19.6% (1e-81)	36.7% (0)	18.1% (1.8e-17)	-
<b>VPS13D</b>	18.8% (1.5e-46)	18.5% (3.7e-48)	18.5% (1.8e-8)	20.4% (7.4e-82)

**Figure S3.** Analysis of similarity in the VPS13 protein family. Identity (%) between human VPS13 family members and *D. discoideum* TipC (calculated using ALIGN program from Biology WorkBench, <http://workbench.sdsc.edu/>) and E-value (shown in brackets) of the best local alignment (LALIGN program from Biology WorkBench, <http://workbench.sdsc.edu/>). Accession numbers are as follows: VPS13A, NP\_150648.2; VPS13B, NP\_060360.3; VPS13C, NP\_001018098.1; VPS13D, NP\_056193.2; TipC, EAL73163.1. Alignment programs from the SDSC Biology WorkBench server (<http://workbench.sdsc.edu/>).